Organic & Biomolecular Chemistry

Cite this: *Org. Biomol. Chem.*, 2012, **10**, 6294

www.rsc.org/obc

PAPER

Theoretical study on the mechanism of Ag-catalyzed synthesis of 3-alkylideneoxindoles from *N*-aryl-α-diazoamides: a Lewis acid or Ag-carbene pathway?†

Zhe Li* and Hai-Xiang Gao

Received 19th March 2012, Accepted 13th June 2012
DOI: 10.1039/c2ob25581b

The mechanism of the title reaction is found to consist of three steps by DFT calculations: (1) N_2 dissociation, (2) intramolecular Ag-carbene addition, and (3) proton transfer. The N_2 dissociation is turnover determining. The product 3-alkylideneoxindole is favored in tautomerization with 3-acetyl-2-hydroxyindole.

Introduction

Transition metal-catalyzed carbene insertion of α-diazocarbonyl compounds into C–H bond is an important method for construction of new C–C bonds in organic synthesis.[1] Although Rh and Cu are the most widely used catalysts for carbene insertion into C–H bonds, Ag complexes have also been found as efficient catalysts with alternative selectivities.[2,3] Intermolecular C(sp^3)–H insertions of *tert*-butanes using α-diazo ester precursors catalyzed by Ag with scorpionate ligands were reported.[4–6] More recently we reported an Ag-catalyzed synthesis of 3-alkylideneoxindoles from diazo compound **1** *via* intramolecular C(sp^2)–H insertion (Scheme 1, eqn (1)).[7] This reaction provides a simple and environmentally benign method to prepare various 3-alkylideneoxindoles which constitute an important class of pharmocophores and metabolic intermediates.[8–12] Previously the Rh-catalyzed cyclization of **1** was reported to produce 3-acetyl-2-hydroxyindole **3** (Scheme 1, eqn (2)).[13,14] However, compound **3** is in fact the same as **2** according to the detailed NMR study in ref. 7. The structural assignment of **3** in ref. 13 and 14 is wrong. Comprehension of the mechanism of eqn (1) may help design methods to improve the efficiency and selectivity of Ag-catalyzed carbene insertion reaction of various diazo compounds.

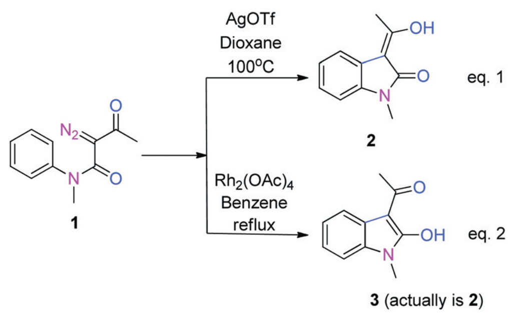

Scheme 1 Indole synthesis from **1**.

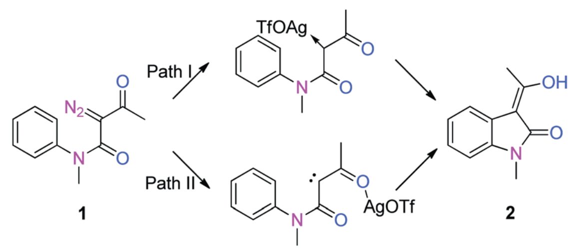

Scheme 2 Ag-carbene and Lewis acid pathways of eqn (1).

The Ag-catalyzed C–H insertion of diazo compounds usually proceeds *via* two possible pathways. In one pathway, Ag promotes N_2 dissociation to form Ag-carbene and then Ag-carbene inserts into the C–H bond (Scheme 2, Path I).[15–17] In the other pathway, Ag facilitates the dissociation of N_2 as a Lewis acid and generates a free carbene to functionalize the C–H bond (Scheme 2, Path II).[18–22] Currently there is little knowledge available to distinguish the above two pathways. Typical Lewis acids such as $FeCl_3$, $TiCl_4$, $BF_3 \cdot Et_2O$, and $SnCl_4$ can also catalyze eqn (1) (albeit in lower yields), indicating that a Lewis acid pathway for Ag catalyst is reasonable.[7] On the other hand, α-methoxycarbonyl Ag-carbene was detected by mass spectrometry as an intermediate in the decomposition of diazomalonates in gas phase.[15] Furthermore, a Rh-carbene mechanism was suggested to be feasible in eqn (2) in Scheme 1.[13] Thus the intermediacy of Ag-carbene cannot be ruled out. To differentiate the two pathways in Scheme 2, the detailed mechanism should be

Department of Applied Chemistry, China Agricultural University, Beijing, China. E-mail: lizhe@cau.edu.cn; Tel: +86-15101058007

† Electronic supplementary information (ESI) available: Computational details, Cartesian coordinates of optimized structures and detailed thermodynamic data. See DOI: 10.1039/c2ob25581b

elucidated. In addition, some other mechanistic questions also need to be answered. For example, how does the Ag complex combine with the substrate and promote N_2 dissociation? Is the C–C formation step carbene insertion or electrophilic substitution? Which step is turnover determining? In order to address above questions, it is necessary to know the structures and energies of key intermediates and transition states of eqn (1). These data can be readily obtained by using modern computational chemistry tools.[23–32]

As our continued efforts to theoretically elucidate the mechanism of transition metal-catalyzed reactions,[33,34] we conducted a detailed computational study on the Ag-carbene pathway and the Ag Lewis acid pathways. The feasible catalytic pathways and the turnover determining step were determined.

Results

N_2 dissociation

N_2 dissociation of **1** produces an Ag-carbene or free carbene which is ready for intramolecular cyclization (Scheme 3). Free substrate **1** and AgOTf are chosen as the reference of free energy calculations of the catalytic cycle. **1** may coordinate to AgOTf with the α-carbon to form **IN1A**, with both the diazo group and one carbonyl to form **IN1B**, or with two carbonyl groups to form **IN1C**. We assume that the three complexes **IN1A**, **IN1B**, and **IN1C** are in fast equilibrium through dissociation and association of **1** to AgOTf. The free energy of **IN1C** (−6.4 kcal mol^{-1}) is the lowest among these three complexes (Fig. 1). Nevertheless, all transition states of N_2 dissociation from **IN1A**, **IN1B**, and **IN1C** need to be considered because an intermediate with higher energy does not necessarily lead to a transition state with a higher activation barrier (Curtin–Hammett principle).

The transition state of N_2 dissociation from **IN1C** is located as **TS1C** with an activation barrier of +33.3 kcal mol^{-1} relative to **IN1C**. The silver stabilized free carbene **IN2B** is produced with a free energy of +3.2 kcal mol^{-1} (Fig. 1). The N_2 dissociation of **IN1B** also produces **IN2B** *via* **TS1B** with an activation barrier of +31.7 kcal mol^{-1} relative to **IN1C**. **IN2B** is a highly reactive singlet free carbene stabilized by the coordination of two carbonyls to AgOTf; however, the activation barrier of **TS1B** or **TS1C** is too high as compared to the barrier of **TS1A**. Thus N_2 dissociation *via* **TS1A** is favored. In addition, the transition state of uncatalyzed N_2 dissociation from **1** is also located as **TS1D** which has an activation barrier of +34.9 kcal mol^{-1}. This is much higher than **TS1A**.

TS1A produces the Ag-carbene complex **IN2A** with a free energy of −9.2 kcal mol^{-1}, which is 12.4 kcal mol^{-1} lower than **IN2B**. The LUMO orbital of **IN2A** is mainly localized on the carbene carbon (Fig. 2), indicating that **IN2A** is an electrophilic Fischer carbene. The bond dissociation energy (BDE) of the Ag–C bond of **IN2A** is 33.7 kcal mol^{-1}. This metal-carbene BDE is significantly lower than those of early transition metal carbenes such as [$(CO)_5M(CH_2)$] (M = W, Cr)[35,36] and *N*-heterocyclic (NHC) Ag-carbenes.[37] The low BDE is consistent with the calculated bond order of Ag–C bond which is 0.49 (NBO) or 0.25 (Mulliken). Frenking *et al.* reported that the Ag–C bond of NHC-Ag carbene is mainly composed of electrostatic attraction (∼65%) and π back bonding (∼20%).[37] The relatively weak Ag–C bond of **IN2A** is presumably due to the weaker σ donating

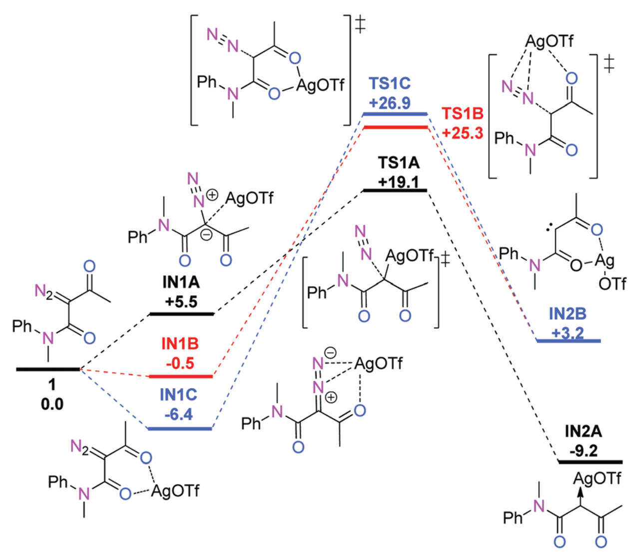

Fig. 1 Free energy profile of N_2 dissociation (kcal mol^{-1}).

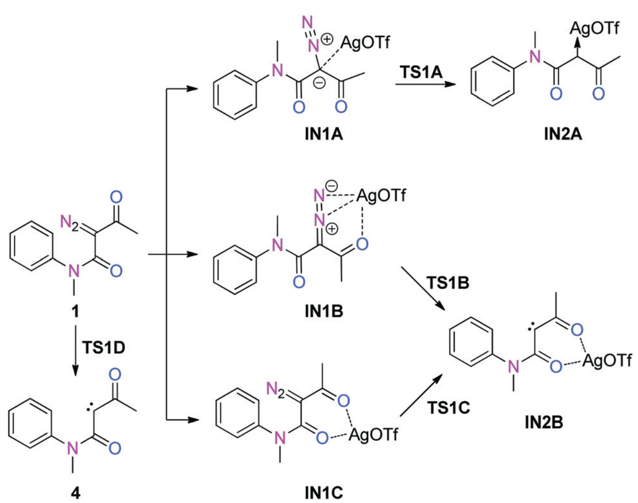

Scheme 3 Pathways of N_2 dissociation.

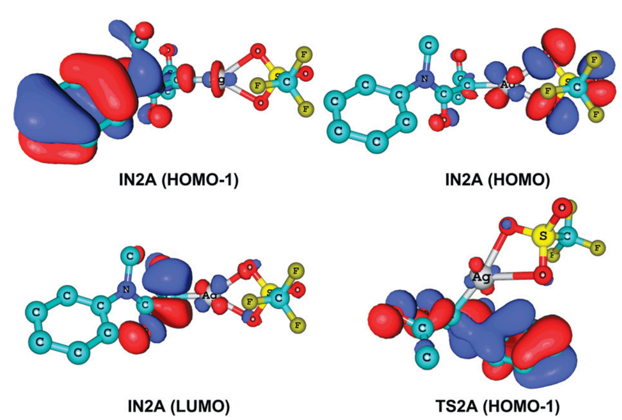

Fig. 2 Molecular orbitals for key intermediates (hydrogen atoms are omitted for clarity, contour value = 0.03).

ability of the carbene moiety of **IN2A** as compared to NHC carbene. The π back bonding in **IN2A** is rather low (see the LUMO of **IN2A** in Fig. 2). Low π back donation was also previously observed in the α-methoxycarbonyl Rh-carbene complex.[31]

In **TS1A**, the positive charge on N_2 decreases from +0.21 (**IN1A)** to +0.16, and the charge of OTf ligand decreases from −0.55 to −0.57. Thus a ligand with a weak ability to accommodate negative charge, *i.e.* low polarizability, should retard the N_2 extrusion step. This is consistent with experimental observations that AgOAc or Ag_2CO_3 are not viable catalysts for the title reaction because the polarizability of a ligand is generally negatively correlated with its basicity.[38]

Cyclization

A careful search for an Ag-carbene insertion transition state in which the new C–C bond and C–H bond are formed simultaneously was not successful (Scheme 4, **TS2B**). Thus a carbene addition pathway is proposed for the cyclization of **IN2A**. A new C–C bond is formed *via* **TS2A** with an activation barrier of only 5.7 kcal mol^{-1} relative to **IN2A** (Fig. 3). The HOMO − 1 orbital of **IN2A** mostly consists of the π-type orbital of the phenyl ring. Thus the C–C bond formation in **TS2A** is due to the interaction between the LUMO and the HOMO − 1 orbitals of **IN2A**, which is observed in the HOMO − 1 orbital of **TS2A** (Fig. 2). The C–C bond formation step is highly exergonic by −30.7 kcal mol^{-1}. A Rh complex similar to **IN3A** was also proposed to account for C–C bond formation in Rh-catalyzed synthesis of 2(3*H*)-indolinones from *N*-aryldiazoamides[14] and in Rh-catalyzed intramolecular carbenoid insertion of biaryldiazoacetates.[39]

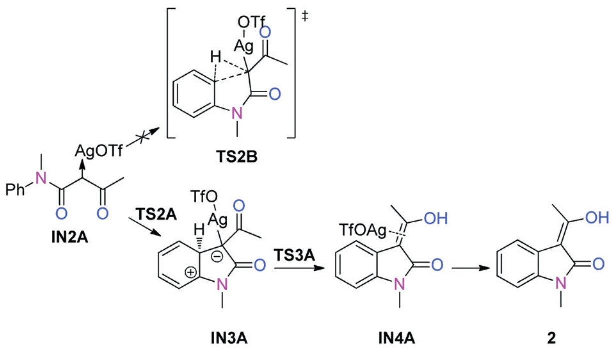

Scheme 4 Pathways of cyclization from **IN2A**.

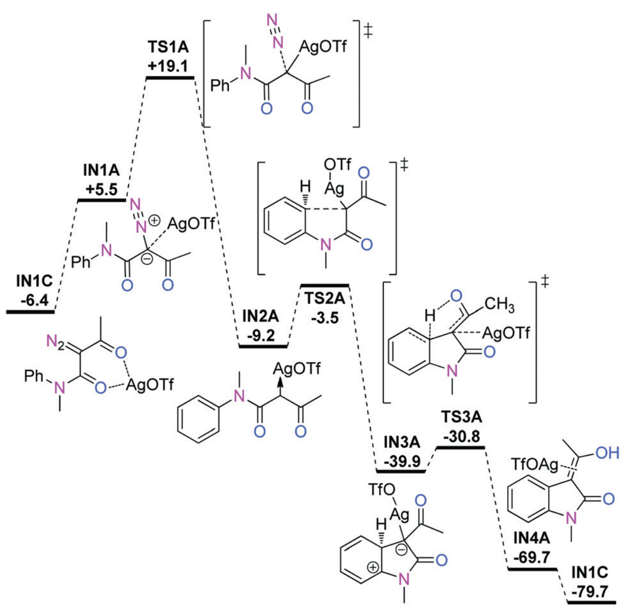

Fig. 3 Free energy profile of the overall catalytic cycle (kcal mol^{-1}).

The H atom on the substituted C of the phenyl ring of **IN3A** is prone to undergoing proton transfer to the acetyl group. The transition state is located as **TS3A** with an activation barrier of 9.1 kcal mol^{-1} relative to **IN3A**. The H atom of **IN3A** could not directly transfer to the O of the amide group because of rigidity of the ring. This indicates that the product of eqn (1) is not **3** but **2** (see below for further discussion). The proton transfer step is exergonic by 29.8 kcal mol^{-1}. The formation of a stable alkylideneoxindole is the major driving force of the proton transfer step. Substitution of **IN4A** by reactant **1** produces the final product **2** and **IN1C** to begin a new catalytic cycle.

The C–H functionalization process is similar to electrophilic substitution of aromatic compounds. Doyle *et al.* proposed a similar mechanism for eqn (2) in Scheme 1.[14] This mechanism is different from Ag or Rh-catalyzed C–H bond activation of alkanes where the carbene directly insert the C–H bond to form the new C–C and C–H bonds in one step.[16,31]

The overall catalytic cycle of the title reaction consists of three main steps, N_2 dissociation, intramolecular Ag-carbene addition, and proton transfer (Fig. 3). **TS1A** is the turnover determining transition state and **IN1C** is the turnover determining intermediate, according to the energetic span model.[40] The energetic span of the catalytic cycle is +25.5 kcal mol^{-1} which is reasonable for a reaction proceeding at 100 °C.[41] The activation barriers of Ag-carbene addition and proton transfer are relatively low. Thus the electronic effect of substituents on the phenyl ring is not observed in the experiment.[7] The overall catalytic reaction is highly exergonic with a reaction free energy of −73.3 kcal mol^{-1}.

Discussion

Catalytic pathway of free carbene IN2B

Other Lewis acids can also catalyze the cyclization of **1** with lower yield. Thus the cyclization pathway of free carbene with AgOTf as Lewis acid is examined in this section (Fig. 4). The activation barrier of N_2 dissociation (**TS1C**) is +33.3 kcal mol^{-1}. **TS2C** is located as the transition state of carbene insertion. The activation barrier of **TS2C** is only 2.4 kcal mol^{-1} higher than **IN2C**. The product of **TS2C** is **IN3B**, with a reaction free energy of −43.7 kcal mol^{-1}. The high activation barrier of N_2 dissociation makes the cyclization of free carbene much less efficient than the Ag-carbene pathway.

Direct production of **IN2B** from **IN1C** is not feasible as shown in Fig. 4. The other possible pathway to generate **IN2B** may be the isomerization of **IN2A**. Indeed, **TS4** is located as the

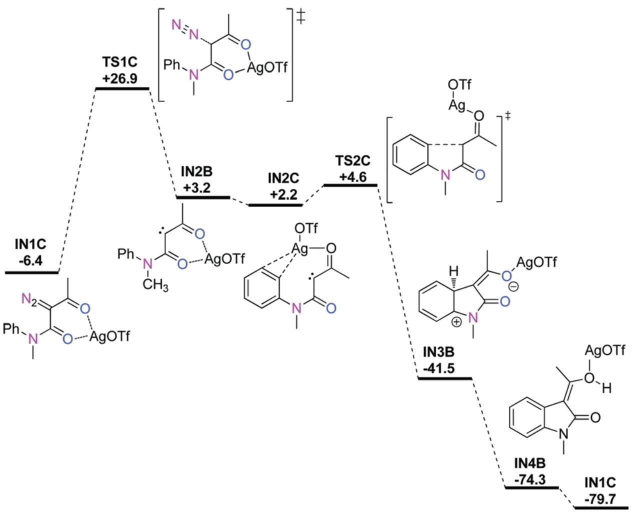

Fig. 4 Reaction pathway of free carbene (kcal mol^{-1}).

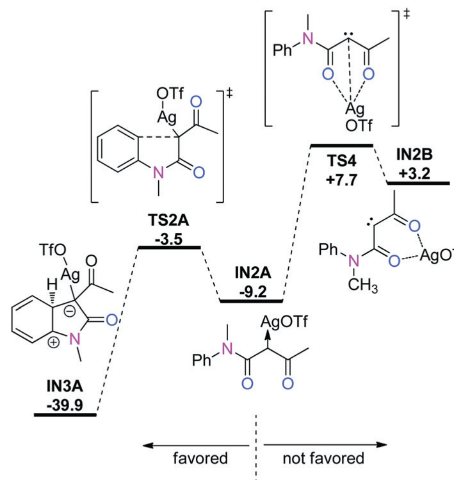

Fig. 5 Two reaction pathways of **IN2A** (kcal mol^{-1}).

transition state for the isomerization between **IN2A** and **IN2B** (Fig. 5). However, the barrier of **TS4** is 11.2 kcal mol^{-1} higher than that of **TS2A**. Thus the cyclization pathway of free carbene is still not favored compared to Ag-carbene pathway.

Tautomerization of compounds 2 and 3

The product of eqn (1) in Scheme 1 is alkylideneoxindole **2** not **3**. One reason is that the proton of **IN3A** could only transfer to the terminal carbonyl due to steric rigidity. Here it is found that **2** is favored in fast equilibrium with **3** *via* intramolecular proton transfer. The transition state of tautomerization is **TS5** with an activation barrier of only +1.9 kcal mol^{-1} (Fig. 6). The transferring H and the two carbonyls are coplanar with H arranged between two oxygens. Thus **2** should be the only observed product in both eqn (1) and (2). This provides further support for the correct structural assignment in ref. 7.

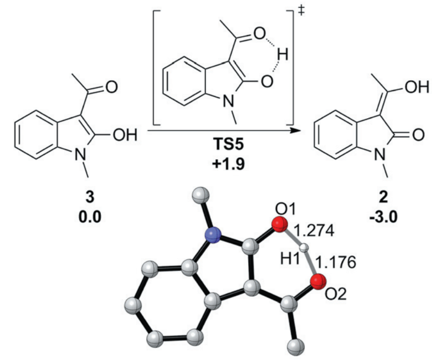

Fig. 6 Tautomerization of **2** and **3** (kcal mol^{-1}).

Conclusions

Ag-catalyzed intramolecular cyclization of *N*-aryl-α-diazoamide is a simple and environmentally benign method for the synthesis of 3-alkylideneoxindoles. In this report, a catalytic pathway involving Ag-carbene complex (**IN2A**) is found to be feasible. The mechanism consists of three main steps, *i.e.* N_2 dissociation, Ag-carbene addition, and proton transfer. The N_2 dissociation step is turnover determining with an activation barrier of +25.5 kcal mol^{-1}. In addition, product **2** is favored in the equilibrium with **3**. Thus **2** should be observed in eqn (1). This is consistent with experimental reports.

Acknowledgements

We thank the NSFC (No. 21002055) and Chinese Universities Scientific Fund (Project No. 2011JS027) for financial support.

Notes and references

1 M. P. Doyle, R. Duffy, M. Ratnikov and L. Zhou, *Chem. Rev.*, 2010, **110**, 704–724.
2 C. J. Lovely, *Silver in Organic Chemistry*, John Wiley & Sons, Inc., 2010, pp. 229–257.
3 Z. Li and C. He, *Eur. J. Org. Chem.*, 2006, 4313.
4 H. V. R. Dias, R. G. Browning, S. A. Richey and C. J. Lovely, *Organometallics*, 2004, **23**, 1200–1202.
5 J. Urbano, T. R. Belderraín, M. C. Nicasio, S. Trofimenko, M. M. Díaz-Requejo and P. J. Pérez, *Organometallics*, 2005, **24**, 1528–1532.
6 C. J. Lovely, R. G. Browning, V. Badarinarayana and H. V. R. Dias, *Tetrahedron Lett.*, 2005, **46**, 2453–2455.
7 H. L. Wang, Z. Li, G. W. Wang and S. D. Yang, *Chem. Commun.*, 2011, **47**, 11336–11338.
8 A. U. Rahman and A. Basha, *Indole Alkaloids*, Harwood Academic Publishers, Amsterdam, 1997.
9 C. V. Galliford and K. A. Scheidt, *Angew. Chem., Int. Ed.*, 2007, **46**, 8748–8758.
10 G. Bartoli, G. Bencivenni and R. Dalpozzo, *Chem. Soc. Rev.*, 2010, **39**, 4449–4465.
11 S. Cacchi and G. Fabrizi, *Chem. Rev.*, 2005, **105**, 2873–2920.
12 S. Cacchi and G. Fabrizi, *Chem. Rev.*, 2011, **111**, PR215–PR283.
13 N. Etkin, S. D. Babu, C. J. Fooks and T. Durst, *J. Org. Chem.*, 1990, **55**, 1093–1096.
14 M. P. Doyle, M. S. Shanklin, H. Q. Pho and S. N. Mahapatro, *J. Org. Chem.*, 1988, **53**, 1017–1022.
15 R. R. Julian, J. A. May, B. M. Stoltz and J. L. Beauchamp, *J. Am. Chem. Soc.*, 2003, **125**, 4478–4486.
16 A. A. C. Braga, F. Maseras, J. Urbano, A. Caballero, M. M. Díaz-Requejo and P. J. Pérez, *Organometallics*, 2006, **25**, 5292–5300.

17 J. Urbano, A. A. C. Braga, F. Maseras, E. Alvarez, M. M. Dıaz-Requejo and P. J. Perez, *Organometallics*, 2009, **28**, 5968–5981.
18 Y. Yue, Y. Wang and W. Hu, *Tetrahedron Lett.*, 2007, **48**, 3975–3977.
19 S. Bachmann, D. Fielenbach and K. A. Jorgensen, *Org. Biomol. Chem.*, 2004, **2**, 3044–3049.
20 W. Kirmse, *Eur. J. Org. Chem.*, 2002, 2193–2256.
21 K. Juhl, R. G. Hazell and K. Anker Jorgensen, *J. Chem. Soc., Perkin Trans. 1*, 1999, 2293–2297.
22 K. Burgess, H.-J. Lim, A. M. Porte and G. A. Sulikowski, *Angew. Chem., Int. Ed. Engl.*, 1996, **35**, 220–222.
23 D. F. Taber, K. K. You and A. L. Rheingold, *J. Am. Chem. Soc.*, 1996, **118**, 547–556.
24 D. T. Nowlan III, T. M. Gregg, H. M. L. Davies and D. A. Singleton, *J. Am. Chem. Soc.*, 2003, **125**, 15902–15911.
25 A. Krapp, K. K. Pandey and G. Frenking, *J. Am. Chem. Soc.*, 2007, **129**, 7596–7610.
26 H. Z. Yu, Y. Y. Jiang, Y. Fu and L. Liu, *J. Am. Chem. Soc.*, 2010, **132**, 18078–18091.
27 S. L. Zhang, Y. Fu, R. Shang, Q. X. Guo and L. Liu, *J. Am. Chem. Soc.*, 2010, **132**, 638–646.
28 S. Zhang, L. Shi and Y. Ding, *J. Am. Chem. Soc.*, 2011, **133**, 20218–20229.
29 Z. Zhang, Y. Liu, L. Ling, Y. Li, Y. Dong, M. Gong, X. Zhao, Y. Zhang and J. Wang, *J. Am. Chem. Soc.*, 2011, **133**, 4330–4341.
30 Z. Y. Lin, J. X. Chen, C. Shi, H. H. Y. Sung, I. D. Williams and G. C. Jia, *Angew. Chem., Int. Ed.*, 2011, **50**, 7295–7299.
31 E. Nakamura, N. Yoshikai and M. Yamanaka, *J. Am. Chem. Soc.*, 2002, **124**, 7181–7192.
32 Y. Liang, H. Zhou and Z.-X. Yu, *J. Am. Chem. Soc.*, 2009, **131**, 17783.
33 Z. Li, S. L. Zhang, Y. Fu, Q. X. Guo and L. Liu, *J. Am. Chem. Soc.*, 2009, **131**, 8815–8823.
34 Z. Li, Y. Fu, S. L. Zhang, Q. X. Guo and L. Liu, *Chem.–Asian J.*, 2010, **5**, 1475–1486.
35 S. F. Vyboishchikov and G. Frenking, *Chem.–Eur. J.*, 1998, **4**, 1428–1438.
36 H. Jacobsen and T. Ziegler, *Inorg. Chem.*, 1996, **35**, 775–783.
37 D. Nemcsok, K. Wichmann and G. Frenking, *Organometallics*, 2004, **23**, 3640–3646.
38 J. O. Edwards, *J. Am. Chem. Soc.*, 1956, **78**, 1819–1820.
39 J.-H. Kim, Y.-H. Ohk, S.-H. Park, Y.-S. Jung and S.-B. Chang, *Chem.–Asian J.*, 2011, **6**, 2040–2047.
40 S. Kozuch and S. Shaik, *Acc. Chem. Res.*, 2011, **44**, 101–110.
41 According to ref. 40, the turnover frequency of a catalytic reaction is calculated by TOF = $(k_B T/h)*\exp(-\Delta G/RT)$ where k_B is Boltzmann constant, T is temperature, h is Planck's constant, and R is the gas constant. Thus the TOF at 100 °C corresponding to 25.5 kcal mol^{-1} is 0.0090 s^{-1} which is in reasonable agreement with the reaction time in ref. 7.